

8-Hydroxy-7-(4-methoxy-phenylazo) quinoline-5-sulfonic acid as corrosion inhibitor for copper in acidic medium

A.S. Fouda¹, S.A. El-Maksod², K. El-Shiekh^{*2}

¹Chemistry Department, Faculty of Science, Mansoura University

²Chemistry Department, Faculty of Science, Port Said University

Received: 9 May 2016/ Accepted: 11 July 2016

*Corresponding author: karimsh240@yahoo.com

Abstract

The Corrosion inhibition of copper in nitric acid has been studied by 8-hydroxy-7-(4-methoxy-phenylazo) quinoline-5-sulfonic acid using weight loss and electrochemical measurements. It was found that the (HQSA) act as a good corrosion inhibitor for copper in all concentrations of the inhibitor. The inhibition action depends on the concentration of the (HQSA) in the acid solution. Results for weight loss and electrochemical measurements indicate that inhibition efficiency increases with increasing inhibitor concentration. Polarization curves revealed that this compound is mixed type inhibitor. The adsorption of (HQSA) on the surface of the copper specimens obeys Temkin adsorption isotherm. Some thermodynamic and kinetic parameters for the corrosion process were estimated, and the values support the results obtained. Some quantum chemical parameters for (HQSA) were calculated.

Keywords: Corrosion, Electrochemistry, Copper, Polarization

Introduction

Copper metallization has been used in integrated circuits for high-speed logic devices instead of the conventional aluminum alloy metallization because of its excellent electrical and thermal conductivity [1-3]. However, it is well known that copper is very susceptible to corrosion in aqueous media and the corrosion products cause a decrease in the electrical conductivity of the devices [4,5]. Thus, much attention has been focused on the behavior of various inhibitors in different media to find the conditions for preventing copper corrosion. Many investigators [6-9] have studied to obtain optimum corrosion protection for copper in various aqueous solutions by either finding new

inhibitors or improving the inhibition efficiency [10]. Most acid corrosion inhibitors are nitrogen, sulfur, or oxygen containing organic compounds. Among these compounds it is generally known that heterocyclic compounds, especially N-based ones, are effective inhibitors the copper corrosion in aqueous solutions [11]. Especially, imidazole and its derivatives are of interest as corrosion inhibitors for copper metal and alloys [12-15].

Imidazole is a planar, aromatic heterocyclic organic compound with two N atoms forming part of a five membered ring [16]. One of the N atoms is of the pyrrole type and the other is a pyridine-like one. Despite extensive studies undertaken on imidazole, until now, it is still questionable what mechanism is adequate for the explanation of the

inhibition of copper corrosion by imidazole in acid solutions.

The objective of this work is to identify four selected 8-hydroxy-7-phenylazo-quinoline-5-sulfonic acid (HQSA) as corrosion inhibitors for copper in 1M HNO₃ by different methods and to analyze the surface morphology of inhibited copper by scanning electron microscope technology with energy dispersive X-ray spectroscopy (SEM-EDX).

2. Experimental.

2.1. Composition of material samples

Table (1): Chemical composition of the copper used in this investigation in weight % as follows:

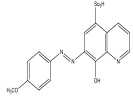
Table (1): The Chemical composition of the copper.

Element	Sn	Ag	Fe	Zn	Pb	As	Cu
Weight %	0.001	0.001	0.01	0.05	0.002	0.0002	The rest

2.2. Chemicals and solutions:

Nitric acid (BDH grade) the organic inhibitor used in this study was synthesized by Anderson et al. [17], and are listed in Table (2).

Table (2): Chemical structure, name, molecular weight and molecular formula of 8-hydroxy-7-(4-methoxy-phenylazo) quinoline-5-sulfonic acid (HQSA).

Compound	Structure	Name	Mol.formula Mol.weight
(HQSA)		8-Hydroxy-7-(4-methoxy-phenylazo) quinoline-5-sulfonic acid	C ₁₆ O ₅ N ₃ H ₁₃ S 359

2.3. Methods used for corrosion measurements.

2.3.1. Weight loss tests:

For weight loss measurements, square specimens of size 2 x 2 x 0.2 cm were used. The specimens were first polished to a mirror finish using 400 up to 1200 grit emery paper, degreased in methanol and finally washed with bidistilled water and dried before being weighed. The specimens then immersed into 100 ml of the test solution. The weight loss measurements were carried out in a 100 ml capacity glass beaker placed in water thermostat. The specimens were then immediately immersed in the test solution

without or with desired concentration of the investigated compound. Triplicate specimens were exposed for each condition and the mean weight losses were reported in order to verify reproducibility of the experiments.

2.3.2. Potentiodynamic polarization measurements.

Polarization experiments were carried out in a conventional three-electrode cell with platinum gauge as the auxiliary electrode and a saturated calomel electrode (SCE) coupled to a fine Luggin capillary as reference electrode. The working electrode was in the form of a square cut from copper sheet of equal composition embedded in epoxy resin of polytetrafluoroethylene so that the flat surface area was 1 cm². Prior to each measurement, the electrode surface was pretreated in the same manner as the weight loss experiments. Before measurements, the electrode was immersed in solution at natural potential for 30 mm until a steady state was reached. The potential was started from - 600 to + 400 mV vs open circuit potential (E_{ocp}). All experiments were carried out in freshly prepared solutions at 30°C and results were always repeated at least three times to check the reproducibility.

2.3.3. Electrochemical impedance spectroscopy measurements.

Impedance measurements were carried out using AC signals of 5 mV peak to peak amplitude at the open circuit potential in the frequency range of 100 kHz to 0.1 Hz. All impedance data were fitted to appropriate equivalent circuit using the Gamry Echem Analyst software.

2.3.4. Electrochemical frequency modulation (EFM) measurements.

EFM experiments were performed with applying potential perturbation signal with amplitude 10 mV with two sine waves of 2 and 5 Hz. The choice for the frequencies of 2 and 5 Hz was based on three arguments [18]. The larger peaks were used to calculate the corrosion current density (I_{corr}), the Tafel slopes (β_c and β_a) and the causality factors CF-2 and CF-3 [19].

All electrochemical experiments were carried out using Gamry instrument PCI300/4 Potentiostat/Galvanostat/Zra analyzer, DC 105

corrosion software, EIS 300 electrochemical impedance spectroscopy software, EFM 140 electrochemical frequency modulation software and Echem Analyst 5.5 for results plotting, graphing, data fitting and calculating.

2.3.6. Theoretical study.

Accelrys (Material Studio Version 4.4) software for quantum chemical calculations has been used.

3. Results and discussion

3.1. Weight loss measurements

Figure (1) represents the weight loss-time curves for copper in 1 M HNO₃ in the absence and presence of different concentrations of (HQSA). Table (3) collects the values of inhibition efficiency (%IE) obtained from weight loss measurements in 1 M HNO₃ at 30 ± 0.1°C. The results of this Table show that the presence of inhibitor reduces the corrosion rate of copper in 1 M HNO₃ and hence, increase the inhibition efficiency.

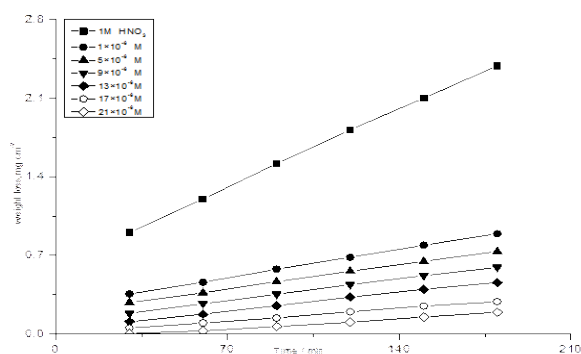


Figure (1): Weight loss-time curves for the dissolution of copper in the absence and presence of different concentrations of (HQSA) at 30°C

Table (3): Inhibition efficiency (%IE) of different concentrations at 30°C from weight loss measurement at 120/min immersion in 1M HNO₃

Compound	Conc., × 10 ⁻⁶ M	C.R. mg cm ⁻² min ⁻¹	% IE
Blank	---	0.01400	---
(HQSA)	1	0.00490	55.6
	5	0.00280	72.9
	9	0.00245	78.5
	13	0.00140	84.2
	17	0.00035	89.3
	21	0.00014	92.5

3.2. Adsorption isotherm.

It is widely acknowledge that adsorption isotherm provide useful insight onto the mechanism of corrosion inhibition as well as the interaction among the adsorbed molecules themselves and their interaction with the electrode surface [20]. In this study, Temkin adsorption isotherm was found to be suitable for the experimental results. The isotherm is described by the following equation:

$$\theta = 2.303/a \log K_{ads} + 2.303/a \log C \quad (1)$$

where C is the inhibitor concentration, K_{ads} is the adsorption equilibrium constant. The plot of θ versus log C gives linear relation (shown in Figure 2). The adsorption equilibrium constant K_{ads}, can be calculated from the intercept and ΔG°_{ads} can be calculated from the following equation:

$$\log K_{ads} = -\log 55.5 - \Delta G^{\circ}_{ad} / 2.303RT \quad (2)$$

where value of 55.5 is the concentration of water in solution in mole/liter [21], R is the universal gas constant and T is the absolute temperature. It was noticed that the value of ΔG°_{ads} , has a negative sign ensure the spontaneity of the adsorption and stability of the adsorbed layer on the alloy surface [22] (Table 4). Values of K_{ads} and ΔG°_{ads} for organic compound were calculated and are recorded in Table (9). In all cases the value of were greater than zero indicating a Temkin adsorption isotherm while the high negative values of ΔG°_{ads} indicate that these derivatives are strongly adsorbed (physorption) on copper surface. K_{ads} were found to run parallel to the % IE. This result reflects the increasing capability, due to structural formation, on the metal surface [23].

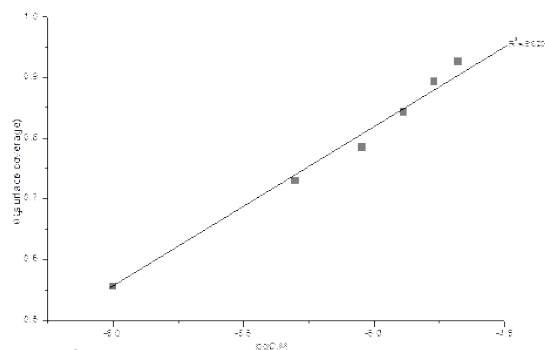


Figure (2): Curve fitting of corrosion data for copper in 1 M HNO₃ in presence of different concentrations of (HQSA) to the Temkin isotherm at 30°C

Table (4): Inhibitor binding constant (K_{ads}), free energy of binding (ΔG°_{ads}) and later interaction parameter (a) for (HQSA) at 30°C.

Compounds	Timkin isotherm		
	a	K_{ads} M ⁻¹	$-\Delta G^{\circ}_{ads}$ KJ mol ⁻¹
(I)	14.0316	1.338	11.5

3.3. Effect of Temperature.

The effect of temperature on the inhibited acid-metal reaction is highly complex, because many changes occur on the metal surface, such as rapid etching and desorption of the inhibitor and the inhibitor itself, in some cases, may undergo decomposition and/or rearrangement. Generally the corrosion rate increases with the rise of temperature. It was found that the inhibition efficiency decreases with increasing temperature and increases with increasing the concentration of the inhibitor. The activation energy (E^*_a) of the corrosion process was calculated using Arrhenius equation [24]:

$$C.R. = A \exp (E^*_a / RT) \quad (3)$$

where C.R. corrosion rate and A is Arrhenius constant The values of activation energies E^*_a can be obtained from the slope of the straight line of plotting $\log C.R.$ vs. $1/T$ in the presence and absence of investigated compound at various temperatures as shown in Figure (3) and in Table (5). It is noted that the values of activation energy increase in the presence of inhibitor and with increase of the concentration of the inhibitor. This is due to the formation of a film of inhibitor on copper surface. The activation energy for the corrosion of copper in 1 M HNO₃ was found to be 51.9 kJ mol⁻¹ which is in good agreement with the work carried out by Fouda et al [25] and others [26,27] An alternative formulation of the Arrhenius equation is the transition state equation (4) [28]:

$$C.R. = RT/Nh \exp (\Delta S^*/R) \exp (-\Delta H^*/RT) \quad (4)$$

where h is Planck's constant, N is Avogadro's number, ΔS^* is the entropy of activation and ΔH^* is the enthalpy of activation. Figure (4) shows a plot of $\log (C.R. / T)$ vs. $(1/T)$. Straight line is obtained with a slope of $(\Delta H^*/2.303 R)$ and an intercept of $(\log R/Nh + \Delta S^*/2.303R)$ from which the values of ΔH^* and ΔS^* are calculated and also listed in Table (4). From inspection of Table (5) it is clear that the positive values of ΔH^* reflect that the process of

adsorption of the inhibitor on the copper surface is an endothermic process; it is attributable unequivocally to chemisorption [29]. Typically, the enthalpy of a physisorption process approaches 100 kJ mol⁻¹. More interesting behavior was observed in Table (5) that positive ΔS^* values is accompanied with endothermic adsorption process. This is agrees with what expected, when the adsorption is an endothermic process, it must be accompanied by an increase in the entropy change and vice versa[30] .

It is seen that investigated compound has inhibiting properties at all the studied temperatures and the values of % IE decrease with temperature increase. This shows that the inhibitor has experienced a significant decrease in its protective properties with increase in temperature. This decrease in the protective properties of the inhibitor with increase in temperature may be connected with two effects; a certain drawing of the adsorption-desorption equilibrium towards desorption (meaning that the strength of adsorption process decreases at higher temperatures) and roughening of the metal surface which results from enhanced corrosion. These results suggest that physical adsorption may be the type of adsorption of the inhibitor on the copper surface.

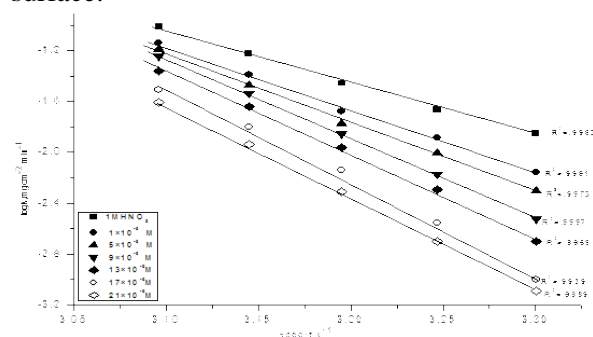
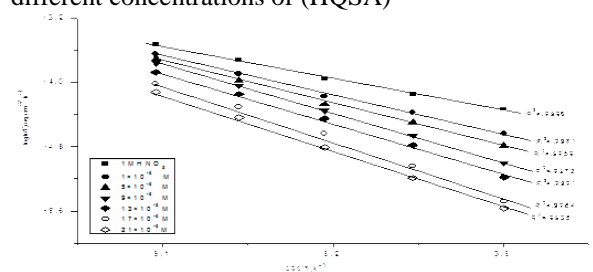
**Figure (3):** $\log k$ (corrosion rate) - $1/T$ curves for copper dissolution in 1M HNO₃ in absence and presence of different concentrations of (HQSA)**Figure (4):** $\log (C.R./T)$ - $(1/T)$ curves for copper dissolution in 1M HNO₃ in absence and presence of different concentrations of (HQSA).

Table (5): Thermodynamic activation parameter for the dissolution of copper in 1M HNO₃ in the absence and presence of different concentrations of investigated (HQSA).

Compound	Conc., x 10 ⁻⁶ M	E _a [*] (KJmol ⁻¹)	ΔH [*] (KJmol ⁻¹)	ΔS [*] Jmol ⁻¹ K ⁻¹
Blank	0.0	79.28	34.9	208.2
(HQSA)	1	113.88	49.44	117.36
	5	124.20	53.88	96.240
	9	143.52	62.28	78.120
	13	150.24	65.16	72.120
	17	168.36	72.60	57.000
	21	167.40	73.08	33.840

3.4. Potentiodynamic polarization measurements.

Theoretically, copper can hardly be corroded in the deoxygenated acid solutions, as copper cannot displace hydrogen from acid solutions according to the theories of chemical thermodynamics [31-33]. However, this situation will change in nitric acid. Dissolved oxygen may be reduced on copper surface and this will allow corrosion to occur. It is a good approximation to ignore the hydrogen evolution reaction and only consider oxygen reduction in the nitric acid solutions at potentials near the corrosion potentials [34]. Polarization measurements were carried out in order to gain knowledge concerning the kinetics of the cathodic and anodic reactions. Figure (5) shows the polarization behavior of copper electrode in 1 M HNO₃ in the absence and presence of various concentrations of (HQSA). Figure (5) shows that both the anodic and cathodic reactions are affected by the addition of investigated organic compound and the inhibition efficiency increases as the inhibitor concentration increases meaning that the addition of inhibitor reduces the anodic dissolution of copper and also retards the cathodic reactions. Therefore, investigated compound is considered as mixed type inhibitor. The values of electrochemical parameters such as corrosion current densities (*I*_{corr}), corrosion potential (*E*_{corr}), the cathodic Tafel slope (β_c), anodic Tafel slope (β_a) and inhibition efficiency (% IE) were calculated from the curves of Fig. 5 and are listed in Table (6).

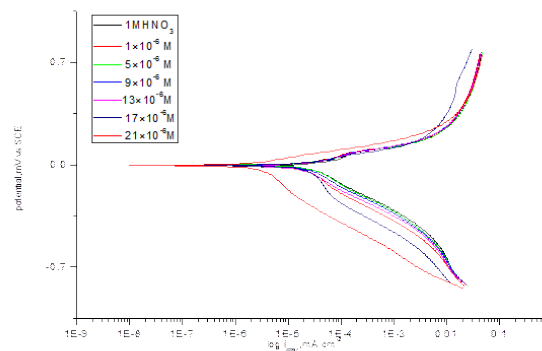


Figure (5): Potentiodynamic polarization curves for the corrosion of copper in 1 M HNO₃ in the absence and presence of various concentrations of (HQSA) at 30°C.

The results in Table (6) revealed that the corrosion current density decreases obviously after the addition of inhibitors in 1 M HNO₃ and % IE increases with increasing the inhibitor concentration. In the presence of inhibitor *E*_{corr} was enhanced with no definite trend, indicating that these compound act as mixed type inhibitor in 1 M HNO₃. The inhibition efficiency and the degree of surface coverage (Θ) were calculated using equation 5:

$$\% \text{ IE}_p = \Theta \times 100 = [1 - (i_{\text{corr}} / i_{\text{corr}}^0)] \times 100 \quad (5)$$

where *i*_{corr}⁰ and *i*_{corr} are the uninhibited and inhibited corrosion current densities, respectively. Also it is obvious from Table (6) that the slopes of the anodic (β_a) and cathodic (β_c) Tafel lines remain almost unchanged upon addition of tested compound, giving rise to a nearly parallel set of anodic lines, and almost parallel cathodic plots results too. Thus, the adsorbed inhibitor act by simple blocking of the active sites for both anodic and cathodic processes. In other words, the adsorbed inhibitor decrease the surface area for corrosion without affecting the corrosion mechanism of copper in 1 M HNO₃ solution, and only causes inactivation of a part of the surface with respect to the corrosive medium [35,36].

Table (6): Effect of concentrations of the investigated (HQSA) on the free corrosion potential (E_{corr}), corrosion current density (i_{corr}), Tafel slopes (β_a & β_c) degree of surface coverage (θ) and inhibition efficiency (% IE) for copper in 1M HNO_3 at 30°C

Compound	Conc., $\times 10^{-6}$ M	$-E_{\text{corr}}$, mV vs SCE	i_{corr} , mA cm^{-2}	β_c mV dec^{-1}	β_a mV dec^{-1}	θ	%IE
Blank	0.0	9.69	8.26	0.3297	0.0956	----	----
(HQSA)	1	1.73	1.872	0.1952	0.0670	0.892	89.2
	5	1.30	1.596	0.1916	0.0651	0.923	92.3
	9	1.14	1.572	0.1878	0.0634	0.925	92.5
	13	0.46	1.440	0.1869	0.0632	0.941	94.1
	17	0.25	1.320	0.1818	0.0622	0.954	95.4
	21	0.18	1.200	0.1782	0.0604	0.967	96.7

3.5 Electrochemical impedance spectroscopy (EIS).

EIS is well-established and powerful technique in the study of corrosion. Surface properties, electrode kinetics and mechanistic information can be obtained from impedance diagrams [37-41]. Figure (6) shows the Nyquist (a) and Bode (b) plots obtained at open-circuit potential both in the absence and presence of increasing concentrations of investigated compound at 30°C. The increase in the size of the capacitive loop with the addition of organic compound shows that a barrier gradually forms on the copper surface. The increase in the capacitive loop size (Figure 6 a) enhances, at a fixed inhibitor concentration. Bode plots (Figure 6 b), shows that the total impedance increases with increasing inhibitor concentration ($\log Z$ vs. $\log f$). But ($\log f$ vs. phase), also Bode plot shows the continuous increase in the phase angle shift, obviously correlating with the increase of inhibitor adsorbed on copper surface. The Nyquist plots do not yield perfect semicircles as expected from the theory of EIS. The deviation from ideal semicircle was generally attributed to the frequency dispersion [42] as well as to the inhomogeneities of the surface. EIS spectra of the tested additive were analyzed using the equivalent circuit, Figure (7), which represents a single charge transfer reaction and fits well with our experimental results. The constant phase element, CPE, is introduced in the circuit instead of a pure double layer capacitor to give a more accurate fit [43]. The double layer capacitance, C_{dl} , for a circuit was calculated by the following relation:

$$C_{dl} = Y_0 \omega^{n-1} / \sin [n (\pi/2)] \quad (6)$$

where Y_0 is the magnitude of the CPE, $\omega = 2\pi f_{\text{max}}$, f_{max} is the frequency at which the imaginary component of the impedance is maximal and the

factor n is an adjustable parameter that usually lies between 0.5 and 1.0. After analyzing the shape of the Nyquist plots, it is concluded that the curves approximated by a single capacitive semicircles, showing that the corrosion process was mainly charged-transfer controlled [45, 46]. The general shape of the curves is very similar for all samples (in presence or absence of inhibitor at different immersion times) indicating that no change in the corrosion mechanism [47]. From the impedance data (Table 7), we conclude that the value of increases with increasing the concentration of the inhibitor and this indicates an increase in % IE, which in concord with the weight loss results obtained. In fact the presence of inhibitor enhances the value of R_{ct} in acidic solution. Values of double layer capacitance are also brought down to the maximum extent in the presence of inhibitor and the decrease in the values of CPE follows the order similar to that obtained for i_{corr} in this study. The decrease in CPE/ C_{dl} results from a decrease in local dielectric constant and/or an increase in the thickness of the double layer, suggesting that organic compound inhibit the copper corrosion by adsorption at metal/acid [48, 49]. The inhibition efficiency was calculated from the charge transfer resistance data from equation (7) [50]:

$$\% IE_{\text{EIS}} = [1 - (R_{ct} / R_{ct}^{\circ})] \times 100 \quad (7)$$

where R_{ct}° and R_{ct} are the charge-transfer resistance values without and with inhibitor respectively.

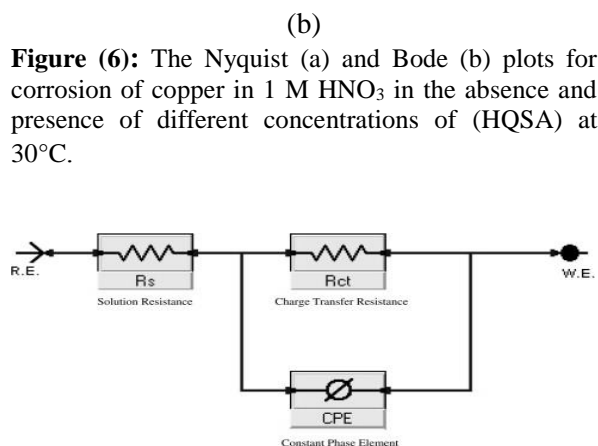
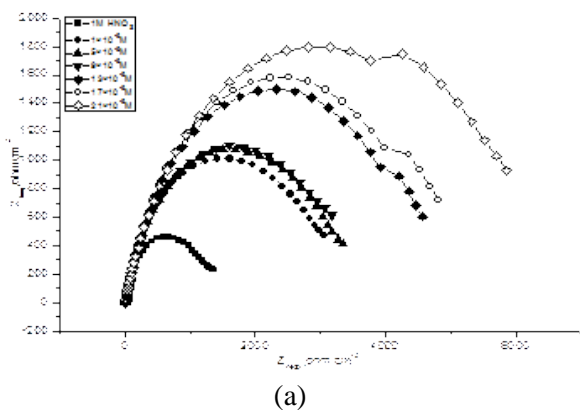


Figure (7): Equivalent circuit model used to fit experimental EIS

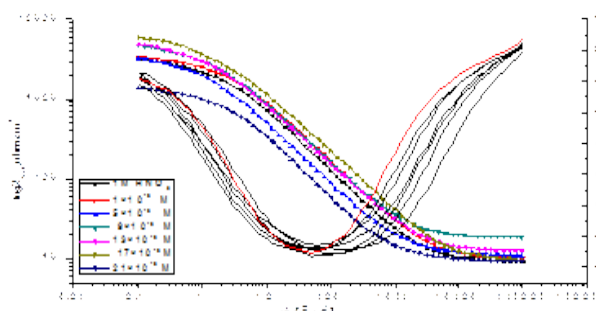


Table (7): Electrochemical kinetic parameters obtained by ETS technique for copper in 1 M HNO₃ without and with various concentrations of (HQSA) at 30°C.

Compound	Conc., x10 ⁻⁶ M	R _s , Ω cm ⁻²	Y ₀ μ Ω ⁻¹ s ⁿ	N	R _{ct} Ω cm ⁻²	C _{dl} μF cm ⁻²	θ	%IE
Blank	0.0	9.41	95.93	810.0	13.24	5.9121	----	----
(HQSA)	1	9.00	46.73	798.1	38.896	2.27264	0.892	89.2
	5	9.72	37.32	791.6	41.808	1.70856	0.923	92.3
	9	11.02	73.91	785.3	42.406	2.39200	0.925	92.5
	13	18.00	41.92	779.3	58.669	2.09272	0.941	94.1
	17	12.27	45.84	774.4	62.218	2.35728	0.954	95.4
	21	8.957	34.78	760.2	74.750	1.67368	0.967	96.7

3.6. Electrochemical Frequency Modulation Technique (EFM).

EFM is a nondestructive corrosion measurement technique that can directly and quickly determine the corrosion current values without prior knowledge of Tafel slopes, and with only a small polarizing signal. These advantages of EFM technique make it an ideal candidate for online corrosion monitoring [51]. The great strength of the EFM is the causality factors which serve as an internal check on the validity of EFM measurement. The causality factors CF-2 and CF-3 are calculated from the frequency spectrum of the current responses.

Figure (8) shows the EFM Intermodulation spectrums of copper in nitric acid solution containing different concentrations of (HQSA). The harmonic and intermodulation peaks are clearly visible and arc much larger than the background noise. The two large peaks, with amplitude of about 200 μA, are the response to the 40 and 100 mHz (2 and 5 Hz) excitation frequencies. It is important to note that between the peaks there is nearly no current response (<100 nA). The experimental EFM data were treated using two different models: complete diffusion control of the cathodic reaction and the “activation” model. For the latter, a set of three non-linear equations had been solved, assuming

that the corrosion potential does not change due to the polarization of the working electrode [52]. The larger peaks were used to calculate the corrosion current density (i_{corr}), the Tafel slopes (β_a & β_c) and the causality factors (CF-2 and CF-3). These electrochemical parameters were listed in Table (8). The data presented in obviously show that, the addition of any one of tested compound at a given concentration to the acidic solution decreases the corrosion current density, indicating that these compound inhibit the corrosion of copper in 1 M HNO_3 through adsorption. The causality factors obtained under different experimental conditions are approximately equal to the theoretical values (2 and 3) indicating that the measured data are verified and of good quality. The inhibition efficiencies $\% \text{IE}_{\text{EFM}}$ increase by increasing the inhibitor concentrations and was calculated as from equation 8:

$$\% \text{IE}_{\text{EFM}} = [1 - (i_{\text{corr}} / i_{\text{corr}}^{\circ})] \times 100 \quad (8)$$

where i_{corr}° , and i_{corr} are corrosion current densities in the absence and presence of inhibitor.

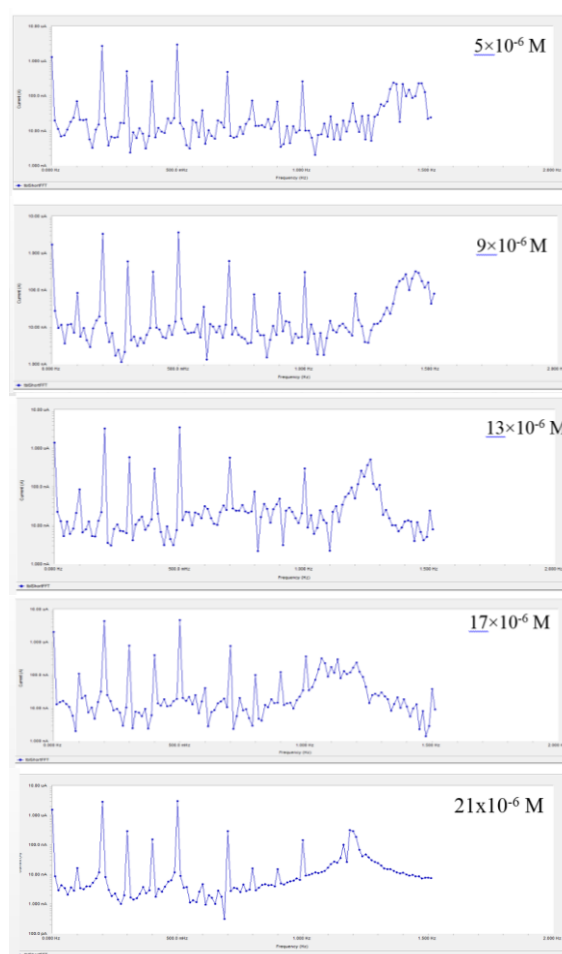
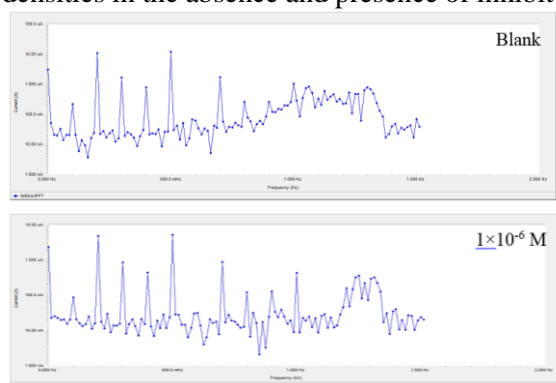


Figure (8): EFM spectra for copper in of 1 M HNO_3 in the absence and presence of different concentrations of (HQSA).

Table (8): Electrochemical kinetic parameters obtained by EFM technique for copper in 1 M HNO_3 without and with various concentrations of (HQSA) at 30°C

Compound	Conc., $\times 10^{-6}$ M	I_{corr} , mA cm^{-2}	β_a mV dec^{-1}	β_c mV dec^{-1}	CF-2	CF-3	ϵ	$\% \text{IE}$
Blank	0.0	17.87	69.82	188.6	1.859	3.644	0.000	00.0
(HQSA)	1	6.1088	65.12	209.1	1.959	4.434	0.892	89.2
	5	5.3272	76.24	392.4	1.963	2.321	0.923	92.3
	9	4.5640	67.72	247.5	1.962	2.045	0.925	92.5
	13	4.4768	56.39	137.6	1.994	3.670	0.941	94.1
	17	3.6640	66.42	237.9	1.929	2.254	0.954	95.4
	21	2.6152	59.62	93.50	1.953	13.42	0.967	96.7

3.8. Quantum chemical calculations.

Figure (11) represents the molecular orbital plots of investigated compound. Theoretical calculations were performed for only the neutral forms, in order to give farther insight into the experimental results. Values of quantum

chemical indices such as energies of lowest unoccupied molecular orbitals (LUMO) and energy of highest occupied molecular orbitals (HOMO) the formation heat ΔH and energy gap ΔE , are calculated by semi-empirical AMI, MNDO and PM3 methods has been given in Table (10). It has been reported that the higher or less negative E_{HOMO} is associated of inhibitor, the

greater the trend of offering electrons to unoccupied orbital of the metal, and the higher the corrosion inhibition efficiency, in addition, the lower E_{LUMO} , the easier the acceptance of electrons from metal surface [54]. due to facilitating of electron transfer between molecular orbital HOMO and LUMO which takes place during its adsorption on the metal surface and thereafter presents the maximum of inhibition efficiency. the adsorption and the inhibition by supporting the transport process through the adsorbed layer. Reportedly, excellent corrosion inhibitors are usually those organic compounds who are not only offer electrons to unoccupied orbital of the metal, but also accept free electrons from the metal [55,56]. It can be seen that all calculated quantum chemical parameters validate these experimental results.

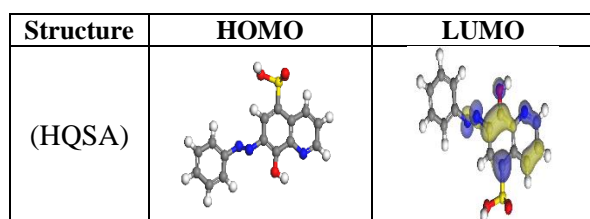


Figure (11): Molecular orbital plots of organic (HQSA).

Table 10. Calculated quantum chemical properties for organic compounds

Parameters	(HQSA)
$E_{HOMO}(eV)$	-9.328
$E_{LUMO}(eV)$	-1.922
$\Delta E(eV)$	6.616
$\eta(eV)$	2.801
$\sigma(eV^{-1})$	0.281
$\Pi(eV)$	-5.742
$X(eV)$	5.920
Dipole moment(Debye)	7.123

3. 9. Inhibition mechanism.

Inhibition of the corrosion of copper in 1 M HNO_3 solution by investigated compound is determined by weight loss, potentiodynamic polarization measurements, electrochemical impedance spectroscopy (ETS) and electrochemical frequency modulation method (EFM), it was found that the inhibition efficiency depends on concentration, nature of metal, the mode of adsorption of the inhibitor and surface conditions. The observed corrosion data in

presence of (HQSA) inhibitor, namely: i) The decrease of corrosion rate and corrosion current with increase in concentration of the inhibitor. ii) The linear variation of weight loss with time. iii) The shift in Tafel lines to higher potential regions. iv) The decrease in corrosion inhibition with increasing temperature indicates that desorption of the adsorbed inhibitor molecules takes place and v) the inhibition efficiency was shown to depend on the number of adsorption active centers in the molecule and their charge density. The corrosion inhibition is due to adsorption of the inhibitor at the electrode! Solution interface, the extent of adsorption of an inhibitor depends on the nature of the metal, the mode of adsorption of the inhibitor and the surface conditions. Adsorption on copper surface is assumed to take place mainly through the active centers attached to the inhibitor and would depend on their charge density. Transfer of lone pairs of electrons on the nitrogen atoms to the copper surface to form a coordinate type of linkage is favored by the presence of a vacant orbital in copper atom of low energy. Polar character of substituents in the changing part of the inhibitor molecule seems to have a prominent effect on the electron charge density of the molecule. It was concluded that the mode of adsorption depends on the affinity of the metal towards the π -electron clouds of the ring system. Metals such as Cu and Fe, which have a greater affinity towards aromatic moieties, were found to adsorb benzene rings in a flat orientation. (HQSA) exhibits excellent inhibition power due to: (i) the presence of p- OCH_3 group which is an electron donating group with negative Hammett constant ($n = -0.268$), Also this group will increase the electron charge density on the molecule and may be an additional active centre (ii) its larger molecular size that may facilitate better surface coverage, and (iii) its adsorption through two active centers a.

References

1. H.Y. Tsai, S.C. Sun, S.J. Wang, J. Electrochem. Soc. 147 (2000)2766.
2. A. Krishnarnoorthy, K. Chanda, S.P. Murarka, G. Ramanath, J.G. Ryan, Appi. Phys. Lett. 78 (2001) 2467.
3. C.E. Ho, W.T. Chen, C.R. Kao, J. Electron. Mater. 30 (2001)379.
4. R.R. Thomas, V.A. Brusic, B.M. Rush, J. Electrochem. Soc. 139(1992) 678.

5. C. Fiaud, Proceedings of the Int. Symposium on Control of Copper and Copper Alloys Oxidation, Rouen, France, (1992) 97.
6. D. Chadwick, T. Hashemi, *Corros. Sci.* 18 (1978) 39.
7. S.L.F.A. da Costa, S.M.L. Agostinho, *J. Electroanal. Chem.* 296(1990) 51.
8. H.A.A. El-Rahman, *Corr.*, 47(1991) 424.
9. N. Bellakhal, K. Draou, A. Addou, J.L. Brisset, *J. Appl. Electrochem.* 30 (2000)595.
10. MM. El-naggar, *J. Mater. Sci.*, 35 (2000) 6189.
11. F. Zucchi, G. Trabanelli, C. Monticelli, *Corr. Sci.*, 38(1996)147.
12. D. Chadwick, T. Hashemi, *Surf. Sci.*, 89(1979)649.
13. S. Yoshida, H. Ishida, *Appl. Surf. Sci.*, 20 (1985)497.
14. M.H. Wahdan, G.K. Gomma, *Mater. Chem. Phys.*, 47(1997)176.
15. S.M. Song, C.E. Park, H.K. Yun, C.S. Hwang, S.Y. Oh, J.M.Park, *J. Adhesion Sci. Tehnol.*, 12 (5) (1998) 541.
16. K. Hofmann *Imidazole and its Derivatives*, Interscience Publishers, Inc, New York, 1953.
17. R. F.Anderson, S. S. Shinde, A.Maroz. *Org. Biomol. Chem.*, 6(2008) 1973.
18. R. W. Bosch, J. Hubrecht, W. F. Bogaerts, B.C. Syrett, *Corr.*, 57(2001)60.
19. S. S. Abdel—Rehim, K. F. Khaled, N. S. Abd—Elshafi, *Electrochim. Acta.*, 51 (2006)6269.
A. N.Wiercinska, G.Dalmate, *Electrochim. Acta.*, 51 (2006) 6179.
20. A.Yurt, A. Balaban, S.U Kandemir., G. Bereket, B.Erk, *Mater Chem. Phys.*, 85(2004) 420.
21. A.Y. Etre, *Appl. Surf. Sci.*, 252(2006) 8521.
A. El-Awady, B. Abd El-Nabey, G. Aziz, *Electrochem.Soc.*, 139 (1992) 2149.
22. G. Trabanelli, in “Corrosion Mechanisms” (Ed. F. Mansfeld) Marcel Dekker, New York., 119 (1987).
A. S. Fouda, A. Abd. E. Aal, A. B. Kandil, *J. Dasalination.*, 201 (2006) 216.
23. F.H. Asaf, M. Abou- Krisha, M. Khodari, F. EL-Cheihk. A. A. Hussien, *Mater Chem. Phys.*, 93 (2002) 1.
A. Fiala, A. Chibani, A. Darchen. A. Boulkarnh, K. Djebbar, *Appl. Surf. Sci.*, 253(2007) 9347.
24. ST. Arab and EM. Noor, *Corr.*, 49 (1993) 122.
25. W. Durnie, R.D. Marco, A. Jefferson, B. Kinsella, *I. Electrochem. Soc.*, 146 (1999) 1751.
26. J.M. Thomas and W.J. Thomas, *Introduction to the Principles of Heterogeneous Catalysis*, 5th Ed, Academic Press, London., (1981) 14.
27. G. Quartarone, G. Moretti, T. Bellomi, G. Capobianco, A. Zingales, *Corro.*, 54(1998)606.
28. W.D. Bjomdahl, K. Nobe, *Corr.*, 40 (1984) 82.
29. Schumacher, A. Muller, W. Stockel, *J. Electroanal. Chem.*, 219 (1987) 311.
30. W.H. Smyrl, in: J.O.M. Bockris, B.E. Conway, E. Yeager, R.E. White (Eds.), *Comprehensive Treatise of Electrochem*, Plenum Press, New York., 4 (1981) 116.
31. G. Quartarone, T. Bellomi, A. Zingales, *Corr. Sci.*, 45 (2003) 722.
32. J.W. Schltze, K. Wippermann, *Electrochim. Acta.*, 32 (1987) 823.
33. D.C. Silverman and J.E. Carrico, *National Association of Corro. Engin.*, 44 (1988) 280.
34. W.J. Lorenz and F. Mansfeld, *Corr. Sci.*, 21(1981) 647.
35. D.D. Macdonald, M.C. Mckubre. “Impedance Measurements in Electroch systems,” *Modern Aspects of Electroch*, J.O’M. Bockris, B.E. Conway, R.E. Whitc, Eds., Plenum Press, New York, New York, .14(1962)8 1.
36. F. Mansfeld; *Corr.*, 36(1981), 301.
37. C. Gabricili, “Identification of Electrochemical processes by Frequency Response Analysis,”*Solartron Instrumentation Group*, 1980.
38. M. El Achouri, S. Kertit, H.M. Gouttaya, B. Nciri, Y. Bensouda, L. Perez, M.R.Jnfante, K. Elkacerni, *Prog. Org. Coat.*, 43 (2001) 267.
39. J.R. Macdonald, W.B. Johanson, in: J.R. Macdonald (Ed.), *Theory in Impedance Spectroscopy*, John Wiley& Sons, New York, 1987.
40. S.F. Mertens, C. Xhoffer, B.C. Decooman, E. Temmerman, *Corrosion* 53 (1997) 381.
41. G. Trabanelli, C. Montecelli, V. Grassi, A. Frignani, *J. Cern. Concr., Res.* 35 (2005) 1804.
A. J. Trowsdate, B. Noble, S .J. Hans, I.S. R. Gibbins, G. E. Thomson, G. C. Wood, *Corr. Sd.*, 38(1996)177.
42. F.M. Reis, H.G. de Melo and I. Costa, *J.Electrochem. Acta.*, 51(2006)17.
43. M. Lagrenee, B. Mernari, M. Bouanis, M. Traisnel & F. Bentiss, *Corros. Sd.*, 44 (2002) 573.

44. E. McCafferty, N. Hackerman, J. Electrochem. Soc., 119 (1972) 146.
45. H. Ma, S. Chen, L. Niu, S. Zhao, S. Li, D. Li, J. Appl. Electrochem 32 (2002) 65.
46. E. Kus, F. Mansfeld, Corr. Sci., 48 (2006) 965.
47. G. A. Caigman, S. K. Metcalf, E. M. Holt, J. Chem. Cryst. 30(2000)415.
48. M. Vajpeyi, S. Gupta, Dharendra and G.N. Pandey, Corr. Prev. Control., October (1985)102.
49. F. Samie, J. Tidblad, V. Kucera, C. Leygraf, 39 (2005) 7362.
50. F. Samie, J. Tidblad, V. Kucera, C. Leygraf., 40, (2006) 363 1.
51. Lukovits, K. Palfi, E. Kalman, Corr., 53(1997)915.